Article

Synthesis of Dicyanovinyl-Substituted 1-(2-Pyridyl)pyrazoles: Design of a Fluorescent Chemosensor for Selective Recognition of Cyanide

Jessica Orrego-Hernández, and Jaime Portilla

J. Org. Chem., **Just Accepted Manuscript** • Publication Date (Web): 24 Nov 2017

Synthesis of Dicyanovinyl-Substituted 1-(2-Pyridyl)pyrazoles: Design of a Fluorescent Chemosensor for Selective Recognition of Cyanide

Jessica Orrego-Hernández and Jaime Portilla*

Bioorganic Compounds Research Group, Department of Chemistry, Universidad de los Andes, Carrera 1 No. 18A-10, Bogotá 111711, Colombia

*Email: jportill@uniandes.edu.co

TOC graphic & Abstract

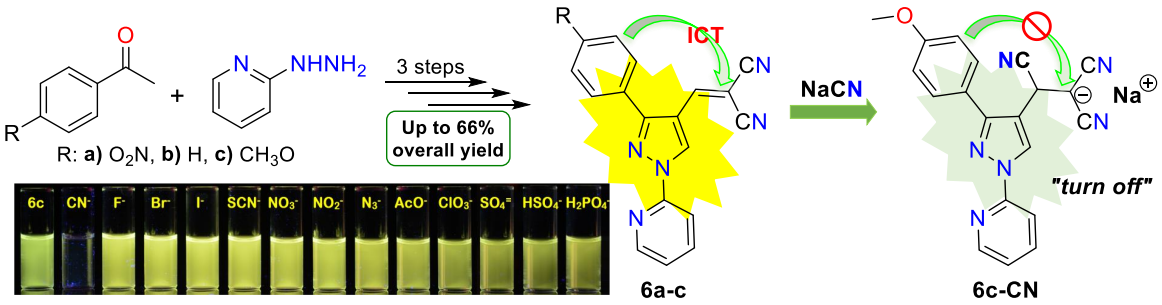

A fluorescence "turn-off" probe have been designed and successfully applied to detect cyanide (CN^-) based on a Michael-type nucleophilic addition reaction and intramolecular charge transfer (ICT) mechanism. For this research, a family of 3-aryl-4-(2,2-dicyanovinyl)-1-(2-pyridinyl)pyrazoles as donor-π-acceptor (D-π-A) systems have been synthesized in 58-66% overall yield, by a three-step synthesis sequence starting from *p*-substituted acetophenones. The product *p*-metoxyphenyl substituted showed good fluorescence emission and large Stokes shifts in different solvents due to its greater ICT. Likewise, this probe evidenced high selectivity and sensitivity, and fast recognition for CN^- with a detection limit of 6.8 µM. HRMS analysis, ^1H NMR titration experiments and TD-DFT calculations were performed to confirm the mechanism of detection and fluorescence properties of the chemodosimeter of CN^-. Additionally, fluorescent test paper was conveniently used to detect cyanide in aqueous solution.

Keywords: Chemosensor, Dicyanovinyl, Fluorescence, 4-Formylpyrazole, Quantum yields

INTRODUCTION

Recently, functionalized pyrazoles have attracted considerable attention due to their proven utility as synthetic intermediates for the preparation of bioactive compounds,[1] fluorescent molecules,[2] and coordination complexes.[3] They have been used to synthesize a great number of *N*-heterocycles with broad spectrum of biological activities,[4] such as antifungal,[4a] antitubercular,[4b] antiviral,[4c] antitumor,[4d] and antiparasitic[4f] activities. Notably, the pyrazole core can act as an electron donor in a chromophoric system due to the presence of an electron-rich nitrogen atom, which is favorable for application in dye chemistry.[5] Tetrasubstituted pyrazoles have been studied with UV-vis and fluorescence spectroscopy showing an intense blue fluorescence and high quantum yields.[6] Also, some pyrazoles are well studied as blue emitters used as electroluminescent materials in organic light-emitting diodes (OLEDs).[7] Due to the broad applications in dye-sensitized solar cell (DSSCs)[8] and second order nonlinear optical devices arylsubstituted, pyrazoles are considered of great interest.[9] In addition, these suitably functionalized heterocycles are used as ligands to chelate metal cations, as well as receptors of anions in the design of fluorescent chemosensors.[10]

On the other hand, cyanide ion is present in water caused by contamination from industrial waste, in cigarette smoke, and in substances present in some foods that releasing it.[11] cyanide in the human bloodstream causes cytotoxic hypoxia and cellular asphyxiation due to the formation of a stable complex with cytochrome *c* oxidase that inhibits the function of this enzyme. In addition, cyanide induces anaerobic metabolism, which leads the lactate accumulation in the blood. The cytotoxic hypoxia and lactate accumulation affect the central nervous system causing respiratory arrest and death.[11-12] Due to the extreme toxicity of cyanide in biological systems, the design of fluorescent probes based on small molecules,[13] metal complexes, [14] polymers,[15] and nanoparticles[16] is of great interest for the sensitive and selective detection of cyanide.[17] For the design of these chemosensors, fundamental photophysical mechanisms such as photoinduced electron transfer (PET), intramolecular charge transfer (ICT), metal–ligand charge transfer (MLCT), twisted intramolecular charge transfer (TICT), and fluorescence resonance energy transfer (FRET) are commonly used.[18]

Consequently, the design of fluorescent probes based on intramolecular charge transfer (ICT) to detect cyanide have been widely studied due to its donor-π-acceptor (D-π-A) properties,

which can be modified favoring fluorescent and colorimetric changes.[19] The dicyanovinyl group is widely used as acceptor moiety in the design of conjugated D-π-A system. Additionally, this acceptor group can react easily with cyanide breaking the conjugation of the D-π-A system who leads the modification of the optical properties of those adducts.[20]

Considering the electron rich and fluorescent properties of the pyrazole derivatives[5-9] and our continuing interest in the synthesis of novel molecules containing this heterocyclic moiety,[1b,21] we proposed the synthesis of a family of 3-aryl-4-(2,2-dicyanovinyl)-1-(pyridin-2-yl)-1*H*-pyrazoles **6a-c** starting from acetophenones **1a-c** (Scheme 1b). These compounds contain a dicyanovinyl group, which acts as acceptor in the design of fluorescent chemosensors.[5,20,22] Pyrazole-4-carbaldehydes **4a-c** play a fundamental role in the achievement of these D-π-A system **6a-c**. The method usually employed in the synthesis of these aldehydes **4'** is based on cyclization-formylation of *N*-arylhydrazones **3'**[23] under the conditions of the Vilsmeier–Haack reaction (Scheme 1a).[5,21e,24]

Scheme 1. Strategy for the Synthesis of 3-Aryl-4-(2,2-dicyanovinyl)pyrazoles.

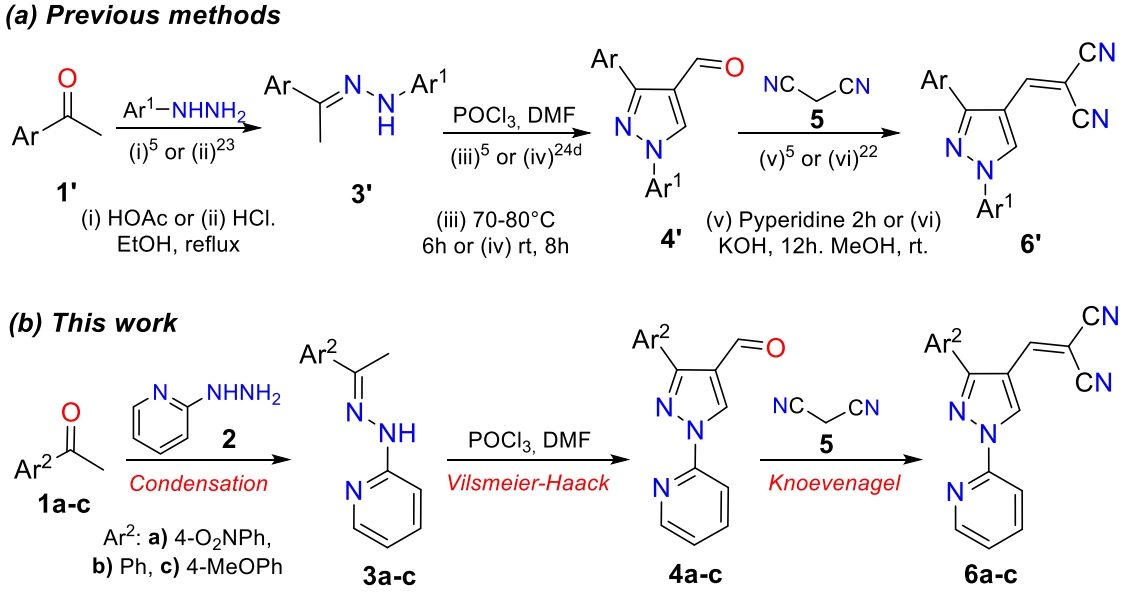

The novel D-π-A system **6a-c** contain an electron rich pyrazole core bound to a dicyanovinyl group (strong acceptor) in position 4 and *p*-substituted aryl group in position 3. The electronic character in *p*-substituted aryl group was modified to evaluate the ICT effect in these structures. In this work, the compound **6c** (*p*-metoxyphenyl substituted) showed better fluorescence

emission in different solvents, and large Stokes shifts due to the ICT is more favored. These results were confirmed by TD-DFT calculations. In addition, the presence of 2-pyridil group on pyrazole moiety of structural analogues of **6a-c** has not yet been reported, which increases the reactivity of electrophilic groups in this structure towards nucleophilic reagents.[21e] Therefore, the detection of cyanide can carried out in short reaction time via a Michael-type nucleophilic addition of cyanide to the dicyanovinyl group on **6c**. Taking in to account this approach, the compound **6c** was studied as a "TURN-OFF" chemodosimeter of cyanide (CN^-) showing a selective detection with a good detection limit in acetonitrile, as well as visual detection of CN^- in paper test. It is important to note that the compound **6c** is the first non-fused pyrazole used as fluorescent chemodosimeter for detection of cyanide.

RESULTS AND DISCUSSION

Synthesis. We started our work by synthesizing 2-(2-(1-arylethylidene)hydrazinyl)pyridines **3a-c**[23] via condensation reaction between acetophenones **1a-c** and 2-hydrazinepyridyne (**2**).[21e] The reaction provided the expected hydrazones **3a-c** as colored solids in 76-92% yields, and without any difficulty in the process. Structure of compounds **3a** was solved by single-crystal X-ray diffraction analysis[25] (see Supporting Information, Figure S1). Subsequently, the synthesis of 3-aryl-1-(pyridin-2-yl)-1*H*-pyrazole-4-carbaldehydes **4a-c** was carried through the cyclization-formylation of Vilsmeier–Haack of the corresponding hydrazone **3a-c**.[24c] All synthesis proceeded efficiently to give the pure 4-formylpyrazole **4a-c**, in 80-85% yields, which indicated the electronic demands of the substituents had little influence on the reactivity, as well as in the synthesis of **3a-c** (Scheme2). However, an impure solid was isolated in the process after aqueous workup, and therefore the product had to be purified by flash chromatography, unlike previous described analogous procedures.[5,21e,24] Probably the presence of 2-pyridil group on the product affect its solubility. The results of these two reaction steps are summarized below (Scheme 3).

Scheme 2. Synthesis of 3-aryl-1-(pyridin-2-yl)-1*H*-pyrazole-4-carbaldehydes **4a-c**.[a]

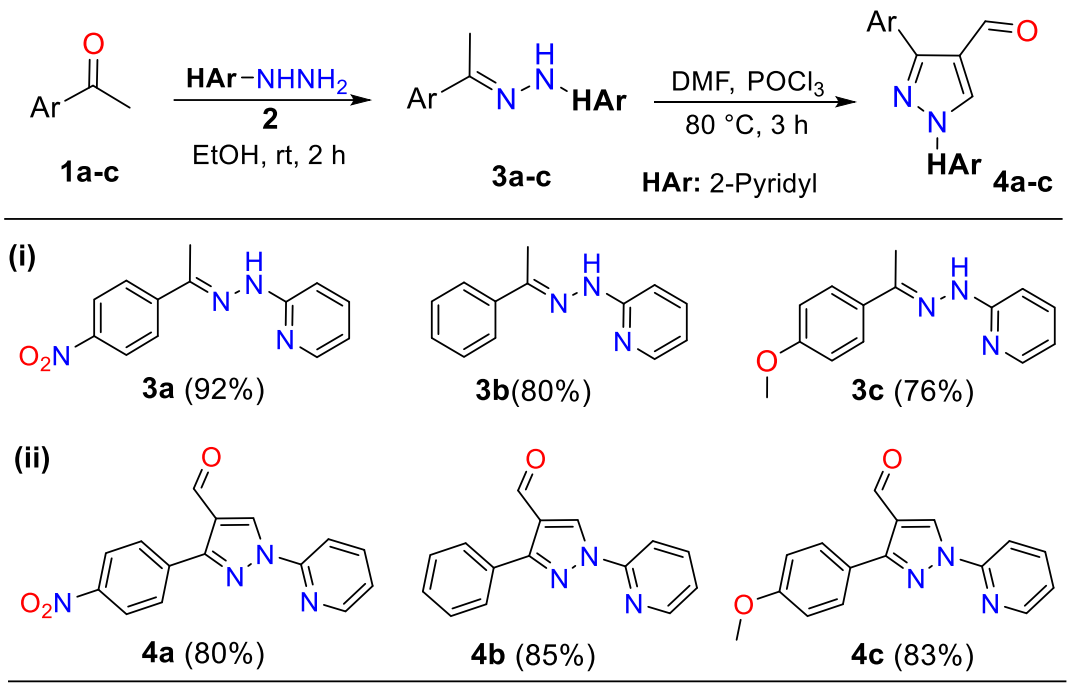

[a] Reaction conditions: (i) **1** (6.00 mmol) and **2** (6.00 mmol) in EtOH (60.0 mL); (ii) DMF (0.6 mL, ~7.5 mmol), $POCl_3$ (1.4 mL, 15.0 mmol) and **3** (2.5 mmol).

Continuing our study regarding the synthesis of the novel D-π-A systems **6a-c**, we decided to carry out the Knoevenagel reaction between those synthesized 4-formylpyrazoles **4a-c** and malononitrile (**5**) according to previous works.[5,20,22] Gratifyingly, the reaction proceeded with operational simplicity and high yields without requiring chromatographic purification. These results allow us to conclude that indeed the presence of 2-pyridil group on **6a-c** increases its reactivity towards nucleophilic reagents. Also, the compound *p*-metoxyphenyl substituted **6c** showed better fluorescence emission (Scheme 3). All reactions offered the pure 3-aryl-4-(2,2-dicyanovinyl)-1-(pyridin-2-yl)-1*H*-pyrazole **6a-c** in 89-92% yield.

Scheme 3. Synthesis of 3-aryl-4-(2,2-dicyanovinyl)-1-(pyridin-2-yl)-1*H*-pyrazole **6a-c**.[a]

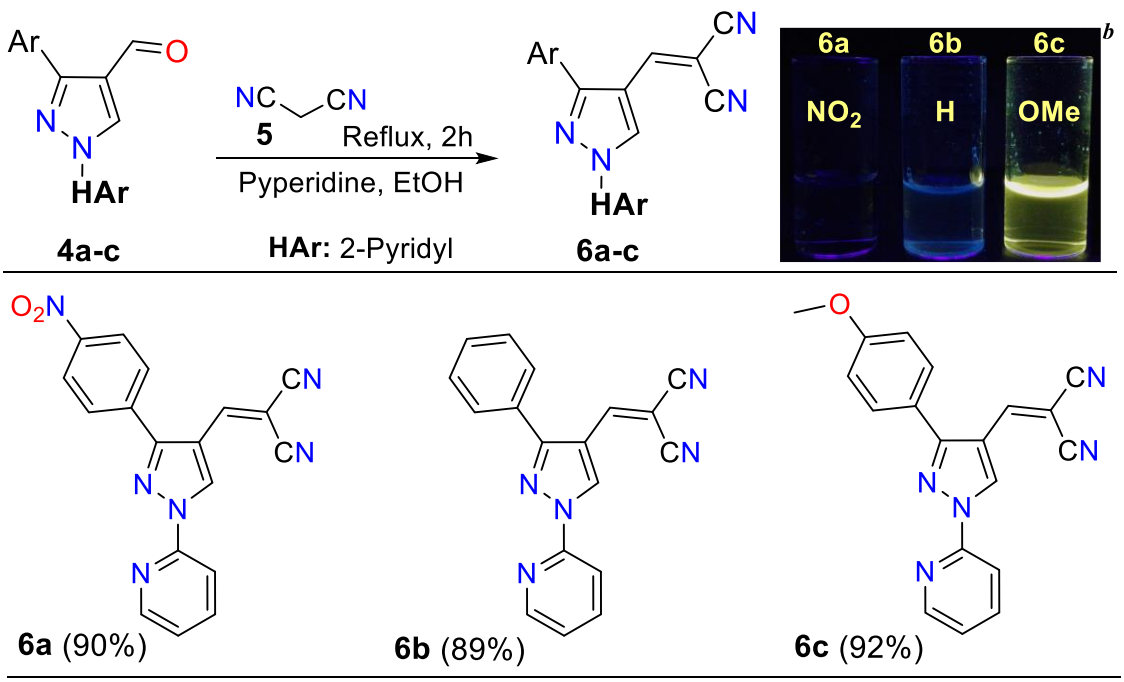

[a] Reaction conditions: **4** (0.50 mmol), **5** (0.50 mmol) and pyperidine (~10 mol %) in EtOH (5.0 mL). [b] Photograph was taken using 10 μM solutions in acetonitrile. A hand-held UV lamp under long wavelength (λ = 365 nm) was used.

The three D-π-A systems **6a-c** were efficiently synthesized in three reaction steps starting from the appropriate *p*-substituted acetophenone **1a-c** and 2-hydrazinepyridyne (**2**). All synthesized compounds (hydrazones **3a-c**, formylpyrazoles **4a-c** and products **6a-c**) were adequately characterized by ^{1}H NMR, ^{13}C NMR, analysis by HRMS and FTIR. The whole carbon skeleton was assigned using ^{13}C NMR spectra, combining with DEPT and two dimensional ^{1}H, ^{13}C shift correlation HSQC and HMBC experiments (see Experimental Section and Supporting Information for details).

Photophysical Properties of 6a-c. The UV-vis and fluorescence emission spectra of the compounds **6a-c** were done in dimethylsulfoxide (DMSO), dimethylformamide (DMF), acetonitrile, ethanol (EtOH), and dichloromethane (DCM), ethyl acetate, and toluene (see Supporting Information, Figures S2-S3 and Table S1). In the UV-vis spectra of **6a-c**, the band between 340-360 nm assigned to charge transfer (CT-bands)[19] is bathochromically shifted by increasing the donating strength of donor group in the order NO_2 < H < MeO. The fluorescence emission of compound **6c** is quite significant *versus* **6a-b** due to the presence of a strong donating group like MeO that favors an higher intramolecular charge-transfer (ICT).[19] The ICT

in **6c** is also responsible of higher Stokes shift and a bathochromic effect of fluorescence spectrums with the increase of solvent polarity (Figure S3). The compound **6c** showed the highest relative quantum yields compared to **6b**, meanwhile **6a** have not fluorescence emission (Table S1). The relative quantum yields (φ_F) of **6c** in DMSO, DMF, EtOH, acetonitrile, DCM, ethyl acetate, and toluene are 0.038, 0.031, 0.014, 0.026, 0.009, 0.118, and 0.022 respectively. Due to the efficient emission fluorescence and large Stokes shift of **6c** in acetonitrile (Figure 1), this solvent was selected in further studies of compound **6c** as a "turn-off" fluorescent chemodosimeter for anions due to the presence of the dicyanovinyl group as a Michael acceptor, where the addition of nucleophile can interrupt the ICT in this compound leading the losing of fluorescence emission.

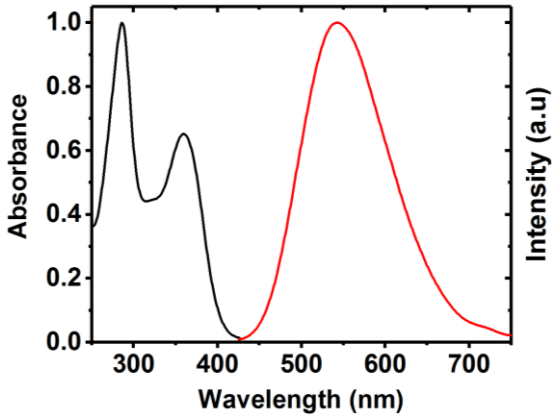

Figure 1. Normalized UV−visible absorption (black line) and fluorescence (red line) spectrum of **6c** in acetonitrile solvent (10 µM). The sample was excited at 360 nm.

Fluorescence and UV-vis Response of 6c to Cyanide (CN^-). Fluorescence spectra of **6c** (50 µM) were taken with an excitation wavelength (λ_{exc}) of 360 nm in acetonitrile to observe the response of fluorescence emission in presence of CN^- and other anions (F^-, Br^-, I^-, SCN^-, NO_3^-, NO_2^-, N_3^-, OAc^-, ClO_3^-, SO_4^{2-}, HSO_4^-, $H_2PO_4^-$, $PO4^{3-}$, and S^{2-}) dissolved in distillated water (Scheme 4 and Figure 2). A substantial diminution of the fluorescence intensity up to 6-fold was observed in presence of one equivalent of CN^- without shifting of the emission band (λ_{em} = 550 nm). In contrast, a small diminution of fluorescence intensity up to less than 1-fold was observed when two equivalents of the other anions were used suggesting that the chemodosimeter **6c** is highly selective towards CN^-. When the UV-vis spectra of **6c** was taken in presence of one equivalent of CN^-, the disappearance of the CT band at 360 nm is almost

completed due to the nucleophilic β-addition of CN^- on the C=C bond of the dicyanovinyl group of **6c**. This addition leads an interruption of the D-π-A system, having a direct influence in the diminution of fluorescence emission (Figure 3).

Scheme 4. Fluorescence response of **6c** in presence of different anions.[a]

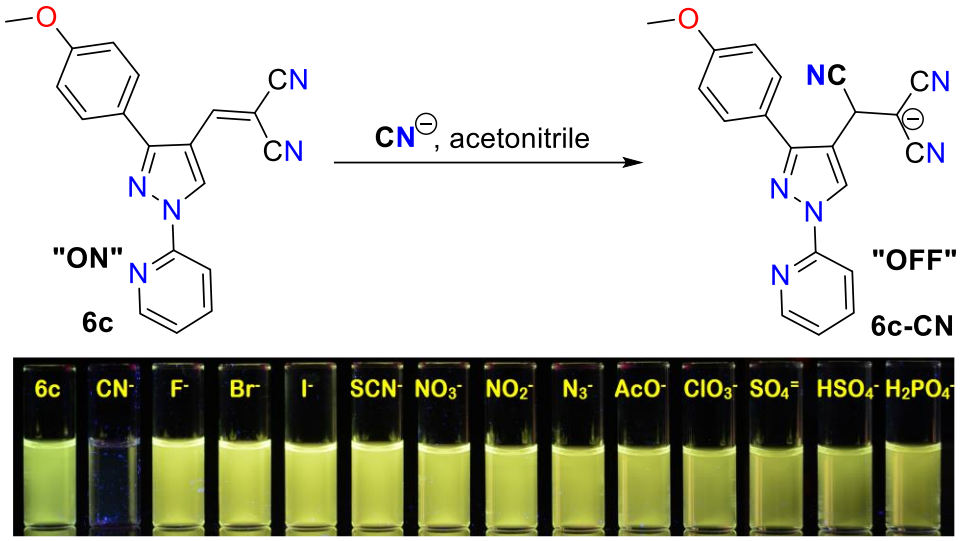

[a] Photograph was taken using 10 μM solutions in acetonitrile-water (1%) and 1.0 equiv of the respective anion. A hand-held UV lamp under long wavelength (λ = 365 nm) was used.

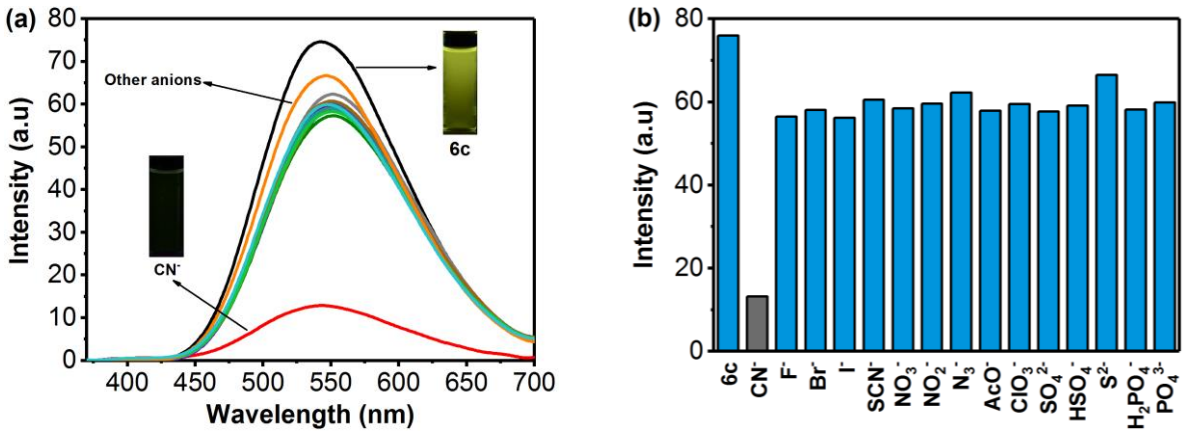

Figure 2. (a) Fluorescence spectra of **6c** (50 μM) in acetonitrile-water (1%) in the presence of 1.0 equiv of CN^- or 2.0 equiv of other anions λ_{exc} = 360 nm. **(b)** Fluorescence intensity response of **6c** to CN^- and other anions.The emission intensity was measured at λ_{em} = 550 nm.

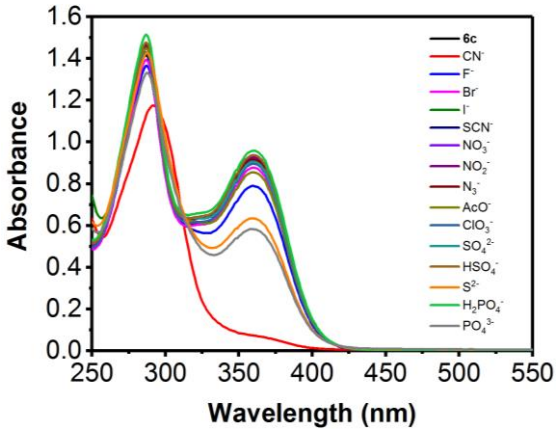

Figure 3. UV-visible absorption spectra of **6c** (50 μM) in acetonitrile-water (1%) in the presence of 1.0 equiv of CN^- or 2.0 equiv of other anions.

On the other hand, UV-vis and fluorescence spectra of **6c** upon addition of one equivalent of CN^- and two equivalents of other anions were measured with the aim to study in more detail the selectivity of **3c** towards CN^-. In these competition experiments, it was found that the S^{2-} anion did not affect the reactivity of CN^- and the other anions had a relatively low interference with exception of HSO_4^-, $H_2PO_4^-$, and PO_4^{3-} on the selectivity for CN^- (see Supporting Information, Figures S4-S5).

In order to understand the response of **6c** towards CN- anion in presence of water, the UV-vis absorption and fluorescence spectra of **6c** were taken by increasing percentage of water in the water-acetonitrile mixtures (see Supporting Information, Figures S6-S7). The UV-vis spectrum of **6c** did not show a significative change until the use of 60 % of water. After the use of 70 % of water the bands at 290 and 360 nm were significantly reduced due to the low solubility of **6c** in water favoring the formation of non-soluble aggregates (Figure S6a). In addition, the fluorescence emission at 550 nm in the spectrum of **6c** showed a gradual diminution of fluorescence intensity with the increment of percentage of water until 60 %. Interestingly, in the range of 70-95 % of water the emission fluorescence spectra were blue shifted to 490 nm with a high emission of fluorescence in comparison with the fluorescence emission of **6c** in pure acetonitrile (Figure S7a). The emission band at 490 nm of **6c** by using 70-95% of water is quite close the band emission of **6c** in solid state (500 nm). This hypsochromic shift and enhancement of fluorescence emission of **6c** in water-acetonitrile solutions between 75-95%

can be explained by aggregation induced emission (AIE) phenomena which is common in dicyanovinyl derivatives.[26]

Furthermore, the UV-vis absorption and fluorescence emission spectra of **6c** with 2 equivalents of CN^- anion at different percentages of water-acetonitrile mixtures were taken (Figures S6b and S7b), where the reactivity of CN^- had not been affected up to of 10 % of water. Between 20 and 60 % of water, for the bands at 360 and 550 nm of compound **6c** in the UV-vis and fluorescence spectra respectively, it had not observed a significant decrease of those bands upon addition of two equivalents of cyanide. The low selectivity of CN^- is due to of solvation of water that interferes in the reactivity of cyanide towards **6c**. For acetonitrile-water solutions of **6c** with 2 equivalents of cyanide between 70 and 95 % of water, the AIE phenomena was principally observed in the fluorescence emission spectra. With these results, it was observed that 10 % of water is the maximal amount of water in acetonitrile-water solutions of **6c** for an optimal detection of cyanide.

Fluorescence and UV-vis spectra of **6c** upon a regular increment of cyanide concentration showed a gradual diminution of fluorescence intensity and absorption bands of 550 and 360 nm respectively (Figures 4-5 and Table S1).

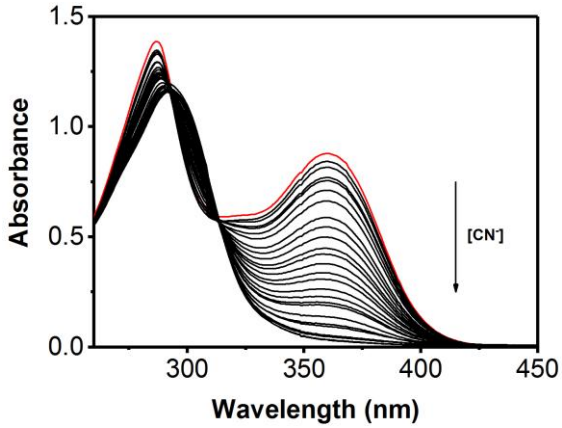

Figure 4. The absorption spectra of **6c** (50 μM) in acetonitrile upon addition of increasing concentrations of CN^- (0-150 μM).

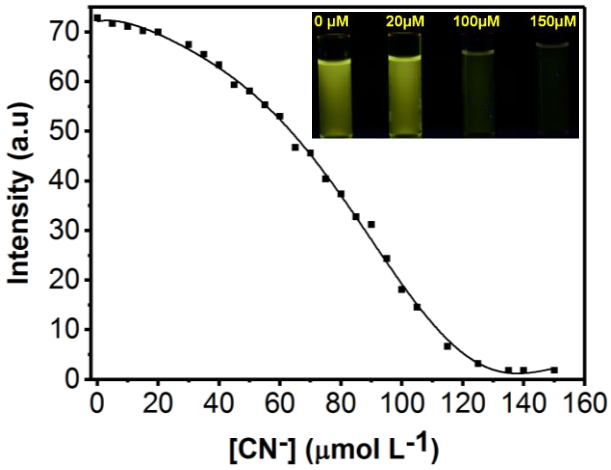

Figure 5. Fluorescence intensity of **6c** at 550 nm with different concentrations of CN^-.

The plot of fluorescence intensity vs concentration of CN^- showed a linear range from 50-105 µM (Figure 6). The detection limit (LOD) was calculated as 6.8 µM (R2 = 0.9921). This LOD is lower than the level goal (MCLG) permitted in drinking water according to USA EPA (0.2 ppm).[27]

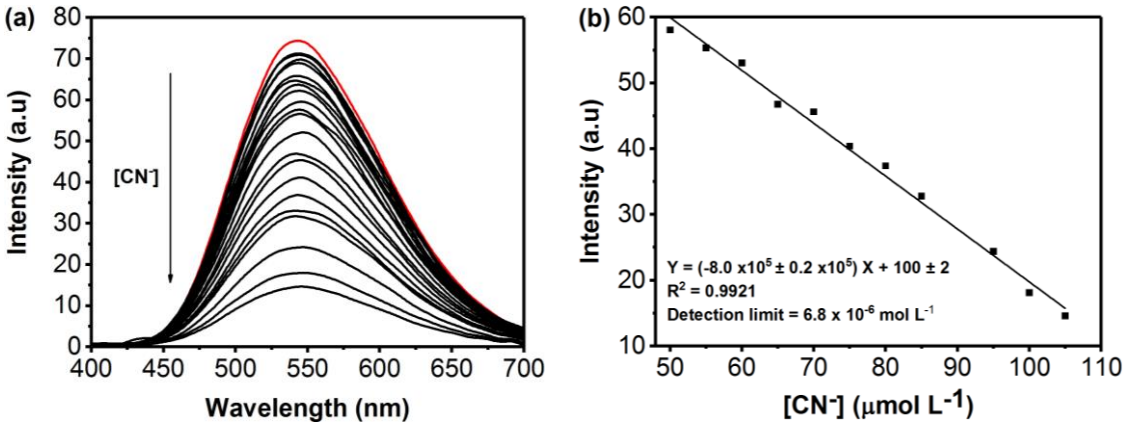

Figure 6. (a) Fluorescence spectra of **6c** (50 µM) in acetonitrile upon addition of increasing concentration of CN^- (0.1–105 µM, λ_{exc} = 360 nm). **(b)** Fluorescence intensity of **6c** at 550 nm with different concentrations of CN^-.

^{1}H NMR titration Experiments and HRMS-ESI Analysis. To demonstrate the reaction process of **6c** with cyanide and the nature of binding site, ^{1}H NMR titration experiment was carried out (Figure 7). During the titration, the concentration of **6c** was kept constant, and the [CN^-]/[**6c**] ratio was increased. Accordingly, upon addition of cyanide to the solution of **6c**, the

Ha signal of the dicyanovinyl group located downfield is shifted to upfield. The protons of the pyridyl group (H1, H2, H3, and H4) are upfield shifted due to the interruption of conjugation and consequent formation of the stabilized carbanion. Additionally, the electrospray ionization mass spectrum (HRMS-ESI) was obtained for the *in situ* intermediate **6c-CN** formed from the compound **6c** and NaCN in acetonitrile, where the peak at m/z 353.1154 is assigned to the negative charge specie [**6c-CN**]$^-$ (Figure 8).

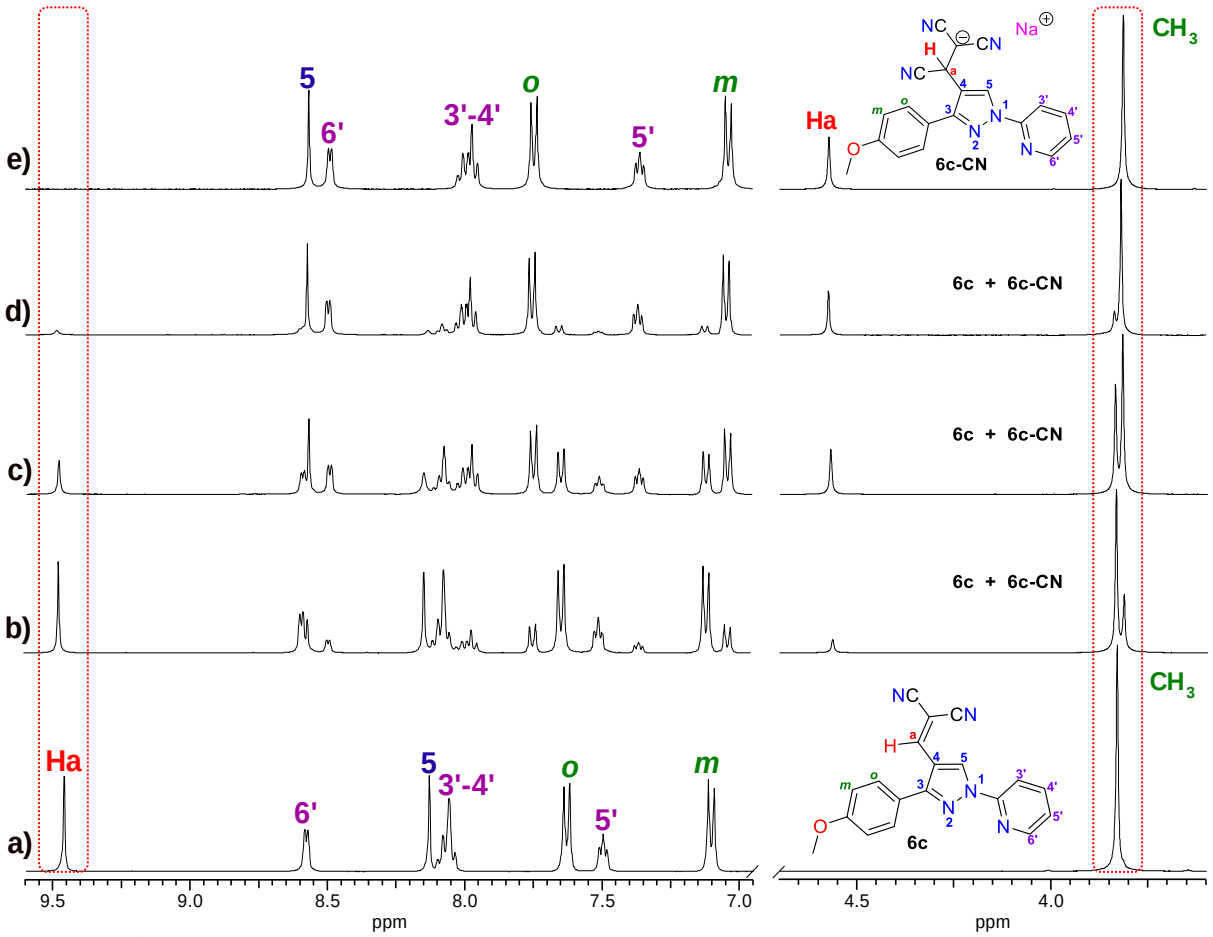

Figure 7. ^{1}H NMR spectra for titration experiment of **6c** using **a)** 0.0, **b)** 0.4, **c)** 0.8, **d)** 1.2, and **e)** 1.6 equiv of NaCN in [D_6]DMSO at room temperature.

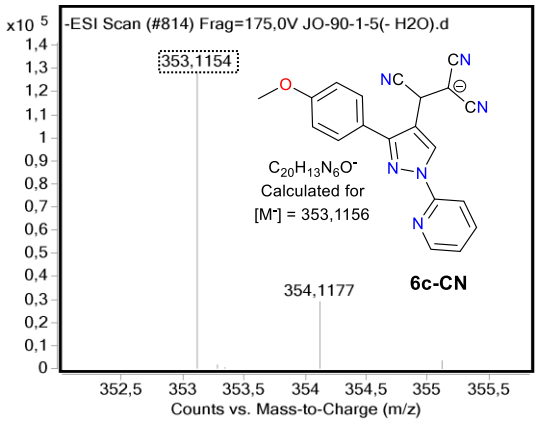

Figure 8. HRMS (ESI) spectrum for the addition adduct of the reaction between **6c** and CN^- in acetonitrile (left) and calculated molecular ion [M^-] of the intermediate 1:1 **6c-CN** (right)

Computational calculation. To have a better understanding about the electronic structures of compounds **6a-c**, TD-DFT calculations were performed at the B3LYP/6-311(d,p) level (Figure 9. Also see Supporting Information, Figures S8-S12 and Table S2).[28] Molecular orbital surfaces of the HOMO and LUMO for the compounds **6a-c** and **6c-CN** are visualized in the Figure 9. In the case of **6a**, the HOMO is located on the 1-(2-pyridyl)-4-dicyanovinylpyrazole system and the LUMO on the *p*-nitrophenyl group. For the contrary, the orbital HOMO in **6b** is distributed on all the molecule and the LUMO on the dicyanovinil group. For the compound **6c** the HOMO is mostly located on the *p*-metoxyphenyl group and the LUMO on the dicyanovinyl moiety. The shape of the two frontier orbitals for **6c** indicates a higher charge transfer (CT) from the electron-donor to the electron-acceptor group in comparison with **6a-b**. The calculated HOMO-LUMO energy gaps for **6a-c** are 3.04, 3.12, and 2.78 eV respectively (see Supporting Information, Figure S9). From these results, the transference of electrons from HOMO to the LUMO is relatively easier in **6c** than in **6a-b**. Thus, in comparison with **6b** a bathochromic shift of **6c** is observed in the electronic absorption spectra (Table S2). These results are consistent with the experimental results.

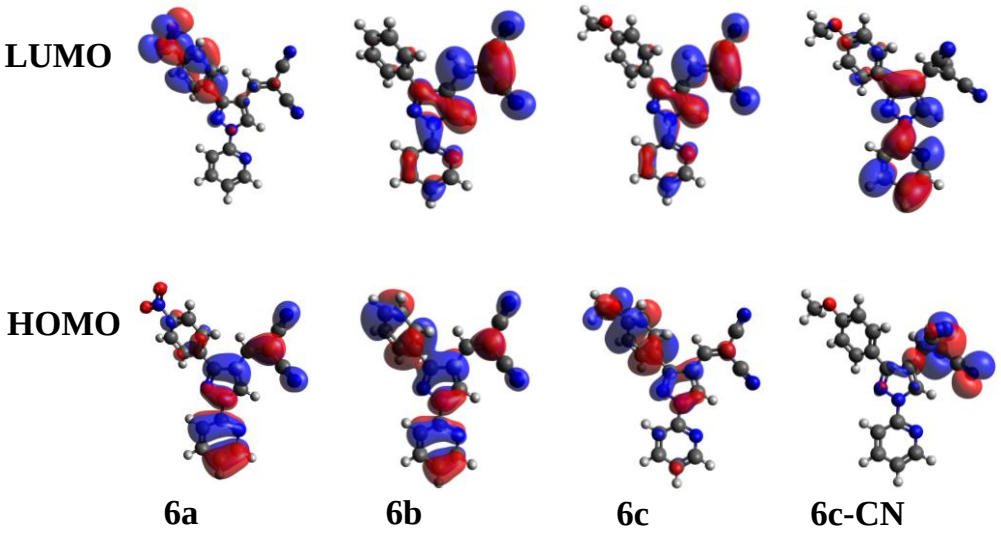

Figure 9. Frontier molecular orbitals of **6a-c** and the adduct **6c-CN** in the ground state

For the adduct **6c-CN** the distribution of the HOMO and LUMO is different in comparison with **6c** (Figure 9). Due to the addition of the CN^- on the dicyanovinyl group, the HOMO of **6c-CN** is confined in that fragment. Thus, the CT from the electron-donor to the electron-acceptor group is interrupted in **6c-CN**, causing a diminution of fluorescence emission. The higher HOMO-LUMO energy gap of **6c-CN (**3.25 eV) compared with **6c** and the absence of the absorption band around 360 nm in the electronic absorption spectra, confirms that, the CT process through donor-π-acceptor system in this compound is disrupted.

Paper Test of 6c for Detection of Cyanide (CN^-). The paper test of the compound **6c** were immersed in aqueous solutions (10 mM) of different anions (I^-, Br^-, F^-, ClO_3^-, NO_3^-, NO_2^-, HSO_4^-, SO_4^{2-}, CN^-, SCN^-, $CH_3CO_2^-$, $H_2PO_4^-$, and N_3^-, where the fluorescence quench was observed selectively in presence of CN^- (Figure 10a). To evaluate the minimal amount of CN^- that the paper strips can detect, different concentrations of CN^- from 0-10 mM were used. This result showed that the minimal concentration of CN^- detectable is 10 mM (Figure 10b). The visual effect of the fluorescent test paper can be used for the selective detection of CN^- in diverse water samples.

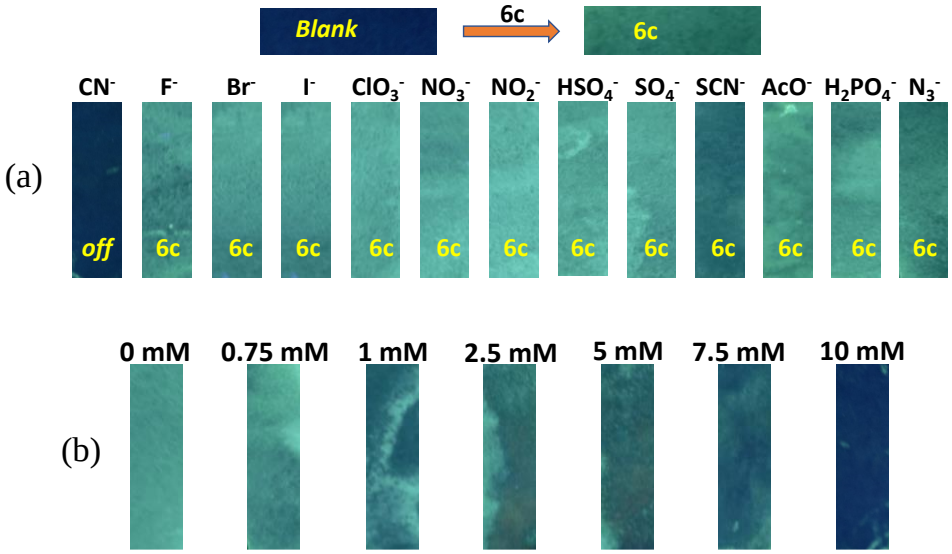

Figure 10. (a) Selective detection of CN^- using the fluorescent test paper of **6c**. (b) Detection of CN^- at different concentration using the fluorescent test paper of **6c**. Photographs were taken using a hand-held UV lamp under long wavelength (λ_{exc} = 365 nm).

CONCLUSIONS

To sum up, we have synthesized a family of 3-aryl-4-(2,2-dicyanovinyl)-1-(pyridin-2-yl)-1*H*-pyrazoles **6a-c** in 58-66% overall yield. The products were obtained in three reaction step (Condensation, Vilsmeier–Haack, Knoevenagel) starting from acetophenones **1**, in high isolated yields at each step. All synthesized compounds were adequately characterized by spectroscopic and HRMS analysis, and the structure of the hydrazone **3a** was confirmed by single-crystal X-ray diffraction analysis. This synthetic methodology could be used to yield other interesting compounds with photophysical and photochemical properties starting from the valuable 4-formyl-1-(2-pyridyl)pyrazoles **4**. Remarkably due to a better intramolecular charge transfer (donor-π-acceptor system) in **6c**, this compound showed a bathochromic shift in the UV-vs absorption spectra, higher fluorescence emission in different solvents, and high Stokes shifts in comparison with its analogs **6a-b**. Therefore, the compound **6c** was studied as a "TURN-OFF" chemodosimeter of CN^-, the results showed a selective detection towards CN^- in comparison with other anions set with a detection limit of 6.8 µM. HRMS analysis and spectroscopic studies like absorption, fluorescence, and NMR spectra revealed the formation of adduct **6c-CN** *via* Michael addition of **CN^-** on the C=C bond of the probe, even ^{1}H NMR

titration experiments were successfully performed. TD-DFT calculations showed the higher charge transfer in the compound **6c** compared with **6a-b**, likewise, an interruption of this ICT in the intermediate **6c-CN**. Essay of fluorescent test paper showed visual selective detection of CN^- anion in aqueous solution (10 mM) that can be applied in the analysis of contaminated water. As a final point, this protocol to design a fluorescent probe with structure analogous to **6c** has not been previously reported. Thus, we expect to extend its use regarding the design of novel fluorimetric and ratiometric chemosensors for anions or even metal ion detection, based in others Michael acceptors like pyrazoles with benzothiazolium salt moiety or in *N*-(2-pyridyl)pyrazole moiety as *N*,*N*-type ligand, respectively.

EXPERIMENTAL SECTION

General Information. All reagents were purchased from commercial sources and used without further purification, unless otherwise noted. All starting materials were weighed and handled in air at room temperature. The reactions were monitored by TLC and visualized using an UV lamp (254 or 365 nm) and/or with *p*-anisaldehyde and H_2SO_4 in EtOH. Flash chromatography was performed on silica gel (230-400 mesh). NMR spectra were recorded at 400 MHz (^{1}H) and 100 MHz (^{13}C) at 298 K using tetramethylsilane (0 ppm) as the internal reference. NMR spectroscopic data were recorded in $CDCl_3$ or [D_6]DMSO using the residual non-deuteriated signal as the internal standards for ^{1}H NMR and the deuteriated solvent signal as the internal standard for ^{13}C NMR spectroscopy. DEPT spectra were used to assign the carbon signals. Chemical shifts (δ) are given in ppm and coupling constants (J) are given in Hz. The following abbreviations are used for multiplicities: s = singlet, d = doublet, t = triplet, and m = multiplet. Melting points were determined using a capillary melting point apparatus and are uncorrected. IR spectra were recorded on a FT-IR spectrophotometer using KBr discs. Spectra are reported in frequency of absorption in cm^{-1}, and only selected resonances are reported. High-resolution mass spectra (HRMS) were recorded using a Q-TOF spectrometer *via* electrospray ionization (ESI). Crystallographic data were recorded on a diffractometer using graphite-monochromated Mo Kα radiation (λ = 0.71073 Å). Structures were solved using an iterative algorithm[29a] and subsequently completed by a difference Fourier map and refined using the program SHELXL2014.[29b] The electronic absorption and fluorescence emission spectra were recorded in quartz cuvettes having a path length of 1 cm. UV-vis and fluorescence measurements were

performed at room temperature (20 ºC). For fluorescence measurements, both the excitation and emission slit widths were 5 nm. Hydrazinylpyridine **2** was prepared using a known procedure.[21e]

Synthesis and Characterization

General Procedure for the Synthesis of 2-(2-(1-Arylethylidene)hydrazinyl)pyridines 3a-c.[23] To a solution of freshly synthesized 2-hydrazinepyridyne (**2**)[21e] (656 mg, 6.0 mmol) in 40 mL of ethanol was added the appropriate acetophenone **1a-c** (6.0 mmol) in 20 mL of ethanol at room temperature. The reaction mixture was stirred at reflux during 2 h. Then the reaction was allowed to cool to room temperature and the solvent was evaporated under reduced pressure. The solid residue was purified by recrystallizetion from ethanol/water to afford the desired hydrazone derivatives **3a-c** as colored solids in good yields.

*2-(2-(1-(4-Nitrophenylethylidene)hydrazinyl)pyridine **3a***. Following the general procedure, for the reaction with 4-nitroacetophenone (**1a**, 992 mg, 6.0 mmol), the hydrazone **3a** was obtained as orange crystals suitable for X-ray diffraction analysis (1416 mg, 92%). Mp 159-160 °C. FTIR: ν = 3421, 3202, 3004, 1584, 1513, 1439, 1323, 1274 cm^{-1}. ^1H NMR ($CDCl_3$, 400 MHz): δ = 2.29 (s, 3H), 6.86 (t, *J* = 6.0 Hz, 1H), 7.43 (d, *J* = 8.5 Hz, 1H), 7.67 (t, *J* = 7.2 Hz, 1H), 7.92 (d, *J* = 9.0 Hz, 2H), 8.16 (d, *J* = 4.1 Hz, 1H), 8.21 (d, *J* = 9.0 Hz, 2H), 8.46 (s, 1H) ppm. $^{13}C\{^1H\}$ NMR ($CDCl_3$, 100 MHz): δ = 2.0 (CH_3), 108.0 (CH), 116.9 (CH), 123.7 (CH), 126.0 (CH), 138.5 (CH), 140.3 (C), 144.6 (C), 147.3 (CH), 156.3 (C) ppm. HRMS (ESI+): calcd. for $C_{13}H_{13}N_4O_2^+$ 257.1039 $[M + H]^+$; found 257.1040.

*2-(2-(1-(Phenylethylidene)hydrazinyl)pyridine **3b***.[23] Following the general procedure, for the reaction with acetophenone (**1b**, 720 mg, 6.0 mmol), the hydrazone **3b** was obtained as yellow crystals (1016 mg, 80%). Mp 139-140 °C (Lit. 138-139 °C).[23] FTIR: ν = 3446, 3204, 3003, 2832, 1595, 1580, 1440, 1244 cm^{-1}. ^1H NMR ($CDCl_3$, 400 MHz): δ = 2.77 (s, 3H), 6.78 (t, *J* = 6.0 Hz, 1H), 7.31-7.44 (m, 4H), 7.62 (t, *J* = 7.3 Hz, 1H), 7.80 (d, *J* = 7.6 Hz, 2H), 8.14 (d, *J* = 4.7 Hz, 1H), 8.30 (s, 1H) ppm. $^{13}C\{^1H\}$ NMR ($CDCl_3$, 100 MHz): δ = 12.3 (CH_3), 107.8 (CH), 115.8 (CH), 125.7 (CH), 128.31 (CH), 138.2 (CH), 138.8 (C), 143.2 (C), 147.2 (CH), 157.1 (C) ppm. HRMS (ESI+) calcd. for $C_{13}H_{14}N_3^+$ 212.1188 $[M + H]^+$; found 212.1191.

2-(2-(1-(4-Methoxyphenylethylidene)hydrazinyl)pyridine ***3c***.[23] Following the general procedure, for the reaction with 4-methoxyacetophenone (**1c**, 900 mg, 6.0 mmol), the hydrazone **3c** was obtained as yellow crystals (1100 mg, 76%). Mp 110-111 °C (Lit. 100-103 °C).[23] FTIR: ν = 3422, 3178, 3011, 2941, 1500, 1439, 1288, 1138 cm^{-1}. ^1H NMR ($CDCl_3$, 400 MHz): δ = 2.24 (s, 3H), 3.84 (s, 3H), 6.76 (t, *J* = 6.0 Hz, 1H), 6.92 (d, *J* = 8.8 Hz, 2H), 7.39 (d, *J* = 8.5 Hz, 1H), 7.60 (t, *J* = 7.5 Hz, 1H), 7.74 (d, *J* = 8.8 Hz, 2H), 8.06 (s, 1H), 8.12 (d, *J* = 4.4 Hz, 1H) ppm. $^{13}C\{^1H\}$ NMR ($CDCl_3$, 100 MHz): δ = 12.2 (CH_3), 55.3 (CH_3), 107.6 (CH), 113.7 (CH), 115.6 (CH), 127.0 (CH), 131.5 (C), 138.2 (CH), 143.1 (C), 147.3 (CH), 157.2 (C), 159.9 (CH) ppm. HRMS (ESI+) calcd. for $C_{14}H_{16}N_3O^+$: 242.1293 $[M + H]^+$; found 242.1288.

General Procedure for the Synthesis of 3-Aryl-1-(pyridin-2-yl)-1*H*-pyrazole-4-carbaldehydes 4a-c. To a flask containing dry *N*,*N*-dimethylformamide (0.58 mL, 7.5 mmol) cooled to 0ºC was added phosphoryl chloride (1.4 mL, 15.0 mmol) for about 1 h maintaining the temperature. The corresponding hydrazone **3a-c** (2.5 mmol) was added, and the mixture was stirred at 80 °C for 3 h. After the completion of the reaction, the mixture was cooled to room temperature, poured into ice-chilled water, and neutralized with 10% sodium bicarbonate solution. The deposited solid was filtered off, washed with cold water and dried under high vacuum to afford the crude product in good yield. The solid residue was purified by flash chromatography on silica gel (eluent: CH_2Cl_2**)** to afford the pure product **4a-c**.

3-(4-Nitrophenyl)-1-(pyridin-2-yl)-1H-pyrazole-4-carbaldehyde ***4a***. Following the general procedure, for the reaction with 2-(2-(1-(4-nitrophenylethylidene)hydrazinyl)pyridine (**3a**, 640 mg, 2.5 mmol), the 4-formylpyrazole **4a** was obtained as a white solid (590 mg, 80%). Mp 209-210 °C. FTIR: ν = 3447, 3153, 3104, 2851, 1687, 1602, 1560, 1456, 1342 cm^{-1}. ^1H NMR ($CDCl_3$, 400 MHz): δ = 7.36 (t, *J* = 6.9 Hz, 1H), 7.93 (t, *J* = 6.9 Hz, 1H), 8.13 (d, *J* = 7.6 Hz, 1H), 8.25 (d, *J* = 8.6 Hz, 2H), 8.34 (d, *J* = 8.6 Hz, 2H), 8.50 (d, *J* = 4.4 Hz, 1H) ppm. $^{13}C\{^1H\}$ NMR ($CDCl_3$, 100 MHz): δ = 113.0 (CH), 122.9 (C), 123.2 (CH), 123.7 (CH), 129.7 (CH), 135.0 (CH), 137.7 (C), 139.2 (CH), 148.2 (C), 148.5 (CH), 150.1 (C), 151.3 (C), 183.5 (CH) ppm. HRMS (ESI+): calcd. for $C_{15}H_{11}N_4O_3^+$ 295.0831 $[M + H]^+$; found 295.0827.

3-(Phenyl)-1-(pyridin-2-yl)-1H-pyrazole-4-carbaldehyde ***4b***.[24d] Following the general procedure, for the reaction with 2-(2-(1-(phenylethylidene)hydrazinyl)pyridine (**3b**, 528 mg, 2.5 mmol), the 4-formylpyrazole **4b** was obtained as a yellow solid (530 mg, 85%). Mp 103-105 °C. FTIR: ν = 3131, 3054, 2848, 2735, 1689, 1596, 1459, 1359, 1192 cm^{-1}. ^1H NMR ($CDCl_3$, 400 MHz): δ = 7.29 (t, *J* = 5.9 Hz, 1H), 7.45-7.53 (m, 3H), 7.86-7.90 (m, 3H), 8.12 (d, *J* = 8.4 Hz, 1H), 8.49 (d, *J* = 4.1 Hz, 1H) ppm. $^{13}C\{^1H\}$ NMR ($CDCl_3$, 100 MHz): δ = 113.1 (CH), 122.5 (C), 122.8 (CH), 128.6 (CH), 128.9 (CH), 129.4 (CH), 131.3 (C), 132.4 (CH), 139.0 (CH), 148.4 (CH), 150.4 (C), 154.7 (C), 184.9 (CH) ppm. HRMS (ESI+): calcd. for $C_{15}H_{12}N_3O^+$ 250.0980 $[M + H]^+$; found 250.0974.

3-(4-Methoxyphenyl)-1-(pyridin-2-yl)-1H-pyrazole-4-carbaldehyde ***4c***. Following the general procedure, for the reaction with 2-(2-(1-(4-methoxyphenylethylidene)hydrazinyl)-pyridine (**3c**, 640 mg, 2.5 mmol), the 4-formylpyrazole **4c** was obtained as a white solid (580 mg, 83%). Mp 102-103 °C. FTIR: ν = 3146, 2967, 2836, 2776, 1675, 1598, 1517, 1474, 1252 cm^{-1}. ^1H NMR ($CDCl_3$, 400 MHz): δ = 3.87 (CH_3), 7.02 (d, *J* = 8.6 Hz, 2H), 7.28 (t, *J* = 6.9 Hz, 1H), 7.85-7.88 (m, 3H), 8.10 (d, *J* = 7.6 Hz, 1H), 8.46 (d, *J* = 4.4 Hz, 1H) ppm. $^{13}C\{^1H\}$ NMR ($CDCl_3$, 100 MHz): δ = 55.3 (CH_3), 113.1 (CH), 114.1 (CH), 122.3 (C), 122.6 (CH), 123.9 (C), 130.2 (CH), 132.8 (CH), 139.0 (CH), 148.3 (CH), 150.4 (C), 154.3 (C), 160.6 (C), 184.8 (CH) ppm. HRMS (ESI+): calcd. for $C_{16}H_{14}N_3O_2^+$ 280.1086 $[M + H]^+$; found 280.1091.

General Procedure for the Synthesis of 3-aryl-4-(2,2-dicyanovinyl)-1-(pyridin-2-yl)-1*H*-pyrazoles 6a-c. To a flask containing an equimolar mixture of 1-(pyridin-2-yl)-1*H*-pyrazole-4-carbaldehyde **4a-c** and malonitrile (**5**, 33 mg, 0.50 mmol) in 5 mL of ethanol was added pyperidine (~10 mol %) as catalyst. The mixture was stirred at reflux for 2 h. Then this was allowed to cool to room temperature and the deposited solid was filtered off, washed with cold ethanol and dried under high vacuum to afford products **6a-c** in high yields.

4-(2,2-Dicyanovinyl)-3-(4-nirophenyl)-1-(pyridin-2-yl)-1H-pyrazole ***6a***. Following the general procedure, for the reaction with 3-(4-nitrophenyl)-1-(pyridin-2-yl)-1*H*-pyrazole-4-carbaldehyde (**4a**, 147 mg, 0.5 mmol), the 4-dicyanovinylpyrazole **6a** was obtained as a white solid (154 mg, 90%). Mp 253-255 °C. FTIR: ν = 3447, 3150, 2231, 1587, 1526, 1463, 1353, 1221 cm^{-1}. ^1H NMR ([D_6] DMSO, 400 MHz): δ = 7.53 (m, 1H), 8.00 (d, *J* = 8.2 Hz, 2H), 8.05-

8.13 (m, 2H), 8.32 (s, 1H), 8.37 (d, *J* = 8.2 Hz, 2H), 8.60 (d, *J* = 4.4 Hz, 1H) ppm. $^{13}C\{^{1}H\}$ NMR ([D_6] DMSO, 100 MHz): δ = 80.2 (C), 113.0 (CH), 122.9 (C), 123.2 (CH), 123.7 (CH), 129.7 (CH), 135.0 (CH), 137.7 (C), 139.0 (CH), 113.8 (C), 113.9 (C), 115.0 (C), 124.0 (CH), 124.1 (CH), 129.2 (CH), 130.3 (CH), 136.3 (C), 140.2 (CH), 147.9 (C), 148.9 (C), 149.1 (CH), 151.7 (CH), 153.0 (CH) ppm. HRMS (ESI+): calcd. for $C_{18}H_{11}N_6O_2^+$ 343.0943 $[M + H]^+$; found 343.0940.

4-(2,2-Dicyanovinyl)-3-(phenyl)-1-(pyridin-2-yl)-1H-pyrazole ***6b***. Following the general procedure, for the reaction with 3-(phenyl)-1-(pyridin-2-yl)-1*H*-pyrazole-4-carbaldehyd*e* (**4b**, 125 mg, 0.5 mmol), the 4-dicyanovinylpyrazole **6b** was obtained as a white solid (132 mg, 89%). Mp 227-228 °C. FTIR: ν = 3447, 3153, 3031, 2228, 1583, 1525, 1463, 1222 cm^{-1}. ^{1}H NMR ($CDCl_3$, 400 MHz): δ = 7.34 (t, *J* = 7.1 Hz, 1H), 7.54-7.58 (m, 5H), 7.78 (s, 1H), 7.90 (t, *J* = 8.0 Hz, 1H), 8.(d, *J* = 8.2 Hz, 1H), 8.52 (d, *J* = 4.8 Hz, 1H) ppm. $^{13}C\{^{1}H\}$ NMR ($CDCl_3$, 100 MHz): δ = 79.9 (C), 113.2 (CH), 113.4 (C), 114.0 (C), 114.9 (C), 123.3 (CH), 129.1 (CH), 129.2 (CH), 129.5 (CH), 129.9 (CH), 130.2 (C), 139.0 (CH), 148.7 (CH), 150.0 (C), 150.9 (CH), 156.5 (C) ppm. HRMS (ESI+): calcd. for $C_{18}H_{12}N_5^+$ 298.1093 $[M + H]^+$; found 298.1092.

4-(2,2-Dicyanovinyl)-3-(4-methoxyophenyl)-1-(pyridin-2-yl)-1H-pyrazole ***6c***. Following the general procedure, for the reaction with 3-(4-methoxyphenyl)-1-(pyridin-2-yl)-1*H*-pyrazole-4-carbaldehyde (**4c**, 140 mg, 0.5 mmol), the 4-dicyanovinylpyrazole **6c** was obtained as a yellow solid (151 mg, 92%). Mp 217-219 °C. FTIR: ν = 3447, 3156, 2226, 1597, 1510, 1463, 1263, 1224 cm^{-1}. ^{1}H NMR ($CDCl_3$, 400 MHz): δ = 3.89 (CH_3), 7.06 (d, *J* = 8.7 Hz, 2H), 7.32 (t, *J* = 7.1 Hz, 1H), 7.49 (d, *J* = 8.7 Hz, 2H), 7.75 (s, 1H), 7.87 (t, *J* = 6.7 Hz, 1H), 8.08 (d, *J* = 8.2 Hz, 1H), 8.50 (d, *J* = 4.0 Hz, 1H) ppm. $^{13}C\{^{1}H\}$ NMR ($CDCl_3$, 100 MHz): δ = 55.5 (CH_3), 79. (C), 113.2 (CH), 113.4 (C), 114.1 (C), 114.7 (CH), 114.8 (C), 122.5 (C), 123.2 (CH), 129.5 (CH), 130.4 (CH), 139.0 (CH), 148.7 (CH), 150.0 (C), 151.2 (CH), 156.3 (C), 161.0 (C) ppm. HRMS (ESI+): calcd. for $C_{19}H_{14}N_5O^+$ 328.1198 $[M + H]^+$; found 328.1199.

Procedure for obtaining Sodium 1,1,2-tricyano-2-(3-(4-methoxyphenyl)-1-(pyridin-2-yl)-1*H*-pyrazol-4-yl)ethan-1-ide 6c-CN. To a NMR tube containing 4-(2,2-dicyanovinyl)-3-(4-methoxyophenyl)-1-(pyridin-2-yl)-*1H*-pyrazole (**6a**, 10 mg, 0.031 mmol) in 0.7 mL of [D_6]

DMSO was added NaCN (0.050 mmol, 1.6 equiv) to afford the adduct **6c-CN** in 100% conversion. ^{1}H NMR ([D$_6$] DMSO, 400 MHz): δ = 3.82 (CH_3), 4.58 (s, 1H), 7.04 (d, *J* = 8.8 Hz, 2H), 7.37 (t, *J* = 6.3 Hz, 1H), 7.75 (d, *J* = 8.8 Hz, 2H), 7.97 (d, *J* = 8.0, 1H), 8.01 (t, *J* = 6.7 Hz, 1H), 8.50 (d, *J* = 4.3 Hz, 1H), 8.57 (s, 1H) ppm. ^{13}C{^{1}H} NMR ([D$_6$] DMSO, 100 MHz): δ = 16.9 (C^-Na^+), 28.1 (CH), 55.3 (CH_3), 111.6 (CH), 114.1 (CH), 118.4 (C), 121.8 (C, CN), 122.1 (CH), 124.5 (C), 126.9 (CH), 128.3 (C, 2CN), 129.2 (CH), 139.8 (CH), 148.5 (CH), 150.3 (C), 150.5 (C), 159.6 (C), 164.8 (C, NaCN) ppm. HRMS (ESI+): calcd. for $C_{20}H_{13}N_6O_2^-$ 353.1156 [M - Na]$^-$; found 353.1154.

Chemosensor Design

UV-vis absorption and fluorescence studies. The solvochromic studies of the compounds **6a-c** were carried out with 0.01 mM stock solutions in dimethylsulfoxide, dimethylformamide, ethanol, acetonitrile, dichloromethane, ethyl acetate, and toluene. The 0.08 mM stock solutions of the chemodosimeter **6c** were prepared in water-acetonitrile (99:1 v/v). The salts used in stock solutions of anions were NaI, KBr, NaF, $NaClO_3$, KNO_3, $NaNO_2$, $NaHSO_4$, Na_2SO_4, NaCN, NaSCN, $NaCH_3CO_2.3H_2O$, NaH_2PO_4, Na_3PO_4, NaN_3, and NaS_2. Inorganic salts were dissolved in distilled water to afford 1 mM aqueous solution. Aliquots of stock solution of **6c** was diluted to 5 mL to make the final concentration of 50 μM. In the selectivity and competition experiments of **6c** towards CN^- and other anions, the fluorescence emission spectra were recorded at λ_{exc} = 360 nm from 50 μM of the chemodosimeter in an acetonitrile solution upon addition of one equivalent of various metal ions. The fluorescence intensities were measured at λ_{em} = 550 nm. Fluorescence response in photographs was excitation at 365 nm using a UV lamp.

Determination of the relative quantum yields. The relative quantum yields were obtained by using anthracene (φ_F = 0.28 in ethanol at 340 nm) as reference and calculated according to the following equation.[30]

$$\varphi_{f,x} = \varphi_{f,st} \cdot \frac{F_x}{F_{st}} \cdot \frac{1 - 10^{-A_{st}}}{1 - 10^{-A_x}} \cdot \frac{\eta_x^2}{\eta_{st}^2}$$

where x and st indicate the sample and standard solution, respectively, φ is the quantum yield, *F* is the integrated area of the emission, *A* is the absorbance at the excitation wavelength, and η is the index of refraction of the solvents.

Determination of the detection limit. The limit of detection (LOD) of **6c** for CN^- was obtained by $3S_b/k$, where S_b is the standard deviation of the blank measurements (by 10 times), and k is the slope from the plot fluorescence intensity *I* versus $[CN^-]$.[30e,31]

DFT calculations Theoretical calculations were obtained using DFT performed using Gaussian 09.[28] The DFT calculations employed the B3LYP hybrid functional and the 6-311G+(d,p) basis set. All geometries were optimized in the ground state without solvent effects. Time-dependent (TD-DFT) calculations were performed on optimized geometries. The visual platform used in this work was Avogadro 1.2.0 to analyze the output files performed in the calculations.[32]

Preparation of test paper

Filter paper was immersed in an acetonitrile solution (1 mM) of compound **6c**, and dried in an oven at 30 ºC for 4 h. The papers were tested in aqueous solutions (10 mM) of different anions (NaI, KBr, NaF, $NaClO_3$, KNO_3, $NaNO_2$, $NaHSO_4$, Na_2SO_4, NaCN, NaSCN, $NaCH_3CO_2.3H_2O$, NaH_2PO_4, and NaN_3 and irradiated with a UV lamp at 365 nm. Additionally, the test papers were studied in aqueous solutions of NaCN varying the concentration from 0-10 mM.

AUTOR INFORMATION

Corresponding Author

∗E-mail: jportill@uniandes.edu.co

ORCID

Jaime Portilla: 0000-0002-8206-7481 786

Notes

The authors declare no competing financial interest.

ACKNOWLEDGEMENTS

The authors are grateful for the financial support from Universidad de los Andes and the Colombian Institute for Science and Research (COLCIENCIAS, project code: 120465843502),

and the High Performance Computing (HPC) services of Vicerrectoria de Investigaciones of Universidad de los Andes. We also acknowledge Edwin Guevara (Universidad de los Andes) for acquiring the mass spectra and Dr. Eduardo C. Escudero-Adan (X-ray Diffraction Unit of Institute of Chemical Research of Catalonia (ICIQ) in Tarragona-Spain) for his help with the analysis of the X-ray crystallographic data.

ASSOCIATED CONTENT

Supporting Information

CIF for compound **3a** and copies of ^{1}H and $^{13}C\{^{1}H\}$ NMR spectra for all compounds, spectroscopic properties and computational calculation of **6a-c** and of **6c-CN**. The Supporting Information is available free of charge on the ACS Publications website at DOI:

REFERENCES

1. (a) Zoppellaro, G.; Enkelmann, V.; Geies, A.; Baumgarten, M. *Org. Lett.* **2014**, *6*, 4929; (b) Quiroga, J.; Portilla, J.; Abonía, R.; Insuasty, B.; Nogueras, M.; Cobo, J. *Tetrahedron Lett*. **2008**, *49*, 5943; (c) Fustero, S.; Román, R.; Sanz-Cervera, J.-F.; Simón-Fuentes, A.; Bueno, J.; Villanova, S. *J. Org. Chem.* **2008**, *73*, 8545; (d) Šenica, L.; Stopar, K.; Friedrich, M.; Grošelj, U.; Plavec, J.; Počkaj, M.; Podlipnik, Č.; Štefane, B.; Svete, J. *J. Org. Chem.* **2016**, *81*, 146; (e) Fricero, P.; Bialy, L.; Brown, A.-W.; Czechtizky, W.; Méndez, M.; Harrity, J.-P.-A. *J. Org. Chem.* **2017**, *82*, 1688.
2. (a) Willy, B.; Müller. T.-J.-J. *Eur. J. Org. Chem*. **2008**, *2008*, 4157; (b) Miniewicz, A.; Palewska, K.; Sznitko, L.; Lipinski, J. *J. Phys. Chem. A* **2011**, *115*, 10689; (c) Götzinger, A.C.; Theßeling, F.-A.; Hoppe, C.; Müller. T.-J.-J. *J. Org. Chem*. **2016**, *81*, 10328.
3. (a) Jarenmark, M.; Fredin, L.-A.; Hedberg, J.-H.-J.; Doverbratt, I.; Persson, P.; Abrahamsson, M. *Inorg. Chem.* **2014**, *53*, 12778; (b) Estevan, F.; Hirva, P.; Ofori, A.; Sanau, M.; Špec, T., Úbeda, M.-A. *Inorg. Chem.* **2016**, *55*, 2101; (c) Burlova, A.-S.; Koshchienkoa, Y.-V.; Makarovaa, N.-I.; Kuz'menkoa, T.-A.; Chesnokova, V.-V., Kiskinb, M.-A.; Nikolaevskiib, S.-A.; Garnovskiic, D.-A.; Uraeva, A.-I.; Vlasenkod, V.-G.; Metelitsaa, A.V. *Synthetic Met*. **2016**, *220*, 543.

4. (a) Harikrishna, N.; Isloor, A. M.; Ananda, K.; Obaid, A.; Fun, H.-K. *RSC Adv.* **2015**, *5*, 43648; (b) Nayak, N.; Ramprasad, J.; Dalimba, U. *Bioorg. Med. Chem. Lett.* **2015**, *25*, 5540; (c) Rashad, A.-E.; Hegab, M.-I.; Abdel-Megeid, R.-E.; Micky, J.-A.; Abdel-Megeid, F.-M.-E. *Bioorg. Med. Chem.* **2008**, *16*, 7102. (d) Li, X.; Lu, X.; Xing, M.; Yang, X.-H.; Zhao, T.-T.; Gong, H.-B.; Zhu, H.-L. *Bioorg. Med. Chem. Lett.* **2012**, *22*, 3589; (e) Rathelot, P.; Azas, N.; El-Kashef, H.; Delmas, F.; Di Giorgio, C.; Timon-David, P.; Maldonado, J.; Vanelle, P. *Eur. J. Med. Chem.* **2002**, *2002*, 671.
5. (a) Miller, R.-D.; Reis, O. *J. Heterocyclic Chem.* **1993**, *30*, 755; (b) Lanke, S. K.; Sekar, N. *Dyes Pigm.* **2016**, *126*, 62; (c) Lanke, S. K.; Sekar, N. *Dyes Pigm.* **2016**, *127*, 116.
6. Willy, B.; Müller, T. J. J. *Org. Lett.* **2011**, *13*, 2082.
7. (a) Ma, C. Q.; Zhang, L. Q.; Zhou, J. H.; Wang, X. S.; Zhang, B. W.; Cao, Y.; Bugnon, P.; Schaer, M.; Nuesch, F.; Zhang, D. Q.; Qiu, Y. *J. Mater. Chem.* **2002**, *12*, 3481; (b) Chen, X.-L.; Yu, R.; Zhang, Q.-K.; Zhou, L.-J.; Wu, X.-Y.; Zhang, Q.; Lu, C.-Z. *Chem. Mater.* **2013**, *25*, 3910.
8. Xia, J.-B.; Li, F.-Y.; Yang, H.; Li, X.-H.; Huang, C.-H. *J. Mater. Sci.* **2007**, *42*, 6412.
9. Mishra, A.; Bhowmik, A. R.; Thakur, M. In *Lasers and Electro-Optics, 1999. CLEO '99. Summaries of Papers Presented at the Conference on* 1999, p 423.
10. (a) Gong, Z.-L.; Zhao, B.-X.; Liu, W.-Y.; Lv, H.-S. *J. Photochem. Photobiol. A* **2011**, *218*, 6; (b) Yang, Z.; Zhang, K.; Gong, F.; Li, S.; Chen, J.; Ma, J. S.; Sobenina, L. N.; Mikhaleva, A. I.; Trofimov, B. A.; Yang, G. *J. Photochem. Photobiol. A* **2011**, *217*, 29; (c) Ciupa, A.; Mahon, M. F.; De Bank, P. A.; Caggiano, L. *Org. Biomol. Chem.* **2012**, *10*, 8753.
11. Kulig, K. W., Cyanide Toxicity, U.S. Department of Health and Human Services, Atlanta, GA, 1991.
12. Nelson, L. *J. Emerg. Nurs.* **2006**, *32*, S8.
13. (a) Jo, J.; Lee, D. *J. Am. Chem. Soc.* **2009**, *131*, 16283; (b) Dong, Y.-M.; Peng, Y.; Dong, M.; Wang, Y.-W. *J. Org. Chem.* **2011**, *76*, 6962; (c) Dong, M.; Peng, Y.; Dong, Y.-M.; Tang, N.; Wang, Y.-W. *Org. Lett.* **2012**, *14*, 130; (d) Hua, Y.-X.; Shao, Y.; Wang, Y.-W.; Peng, Y. *J. Org. Chem.* **2017**, *82*, 6259.
14. (a) Lou, X.; Ou, D.; Li, Q.; Li, Z. *Chem. Commun.* **2012**, *48*, 8462; (b) Guo, Y.-Y.; Tang, X.-L.; Hou, F.-P.; Wu, J.; Dou, W.; Qin, W.-W.; Ru, J.-X.; Zhang, G.-L.; Liu, W.-S.; Yao, X.-J. *Sens. Actuator B-Chem.* **2013**, *181*, 202; (c) Shaily; Kumar, A.; Ahmed, N. *Ind. Eng. Chem. Res.* **2017**, *56*, 6358.

15. (a) Lin, Q.; Zhong, K.-P.; Zhu, J.-H.; Ding, L.; Su, J.-X.; Yao, H.; Wei, T.-B.; Zhang, Y.-M. *Macromolecules* **2017**, *50*, 7863; (b) Trigo-López, M.; Muñoz, A.; Mendía, A.; Ibeas, S.; Serna, F.; García, F. C.; García, J. M. *Sens. Actuator B-Chem.* **2018**, *255*, 2750
16. (a) Shojaeifard, Z.; Hemmateenejad, B.; Shamsipur, M. *ACS Appl. Mater. Interfaces* **2016**, *8*, 15177; (b) Dong, Z.-Z.; Yang, C.; Vellaisamy, K.; Li, G.; Leung, C.-H.; Ma, D.-L. *ACS Sens.* **2017**, *2*, 1517.
17. Wang, F.; Wang, L.; Chen, X.; Yoon, J. *Chem. Soc. Rev.* **2014**, *43*, 4312.
18. (a) Keshav, K.; Torawane, P.; Kumar Kumawat, M.; Tayade, K.; Sahoo, S. K.; Srivastava, R.; Kuwar, A. *Biosens. Bioelectron.* **2017**, *92*, 95; (b) Thanayupong, E.; Suttisintong, K.; Sukwattanasinitt, M.; Niamnont, N. *New J. Chem.* **2017**, *41*, 4058; (c) Bar, M.; Maity, D.; Das, K.; Baitalik, S. *Sens. Actuator B-Chem.* **2017**, *251*, 208; (d) Xie, Z.; Kong, X.; Feng, L.; Ma, J.; Li, Y.; Wang, X.; Bao, W.; Shi, W.; Hui, Y. *Sens. Actuator B-Chem.* **2018**, *257*, 154; (e) Prakash, K.; Ranjan Sahoo, P.; Kumar, S. *Dyes Pigments* **2017**, *143*, 393.
19. Bures, F. *RSC Adv.* **2014**, *4*, 58826.
20. (a) Cheng, X.; Tang, R.; Jia, H.; Feng, J.; Qin, J.; Li, Z. *ACS Appl. Mater. Interfaces.* **2012**, *4*, 4387; (b) Chen, W.; Zhang, Z.; Li, X.; Agren, H.; Su, J. *RSC Adv.* **2015**, *5*, 12191.
21. (a) Quiroga, J.; Portilla, J.; Abonia, R.; Insuasty, B.; Nogueras, M.; Cobo, J. *Tetrahedron Lett.* **2007**, *48*, 6352; (b) Quiroga, J.; Portilla, J.; Abonia, R.; Insuasty, B.; Nogueras, M.; Cobo, J. *Tetrahedron Lett.* **2008**, *49*, 6254; (c) Portilla, J.; Quiroga J.; Abonía, R.; Insuasty, B.; Nogueras, M.; Cobo, J.; Mata, E. *Synthesis* **2008**, *3*, 387; (d) Portilla, J.; Quiroga, J.; Nogueras, M.; Cobo, J. *Tetrahedron* **2012**, *68*, 988; (e) Orrego-Hernández, J.; Cobo, J.; Portilla, J. *Eur. J. Org. Chem.* **2015**, *2015*, 5064; (f) Castillo, J.-C.; Estupiñan, D.; Nogueras, M.; Cobo, J.; Portilla, J. *J. Org. Chem.* **2016**, *81*, 12364. (g) Castillo, J.-C.; Rosero, H.-A.; Portilla, J. *RSC Adv.* **2017**, *7*, 28483.
22. El-Shishtawy, R.-M.; Al-Zahrani, F.-A.-M.; Al-amshany, Z.-M.; Asiri, A.-M. *Sens. Actuator B-Chem.* **2017**, 240, 288.
23. Todeschini, A.-R.; De Miranda, A.-L.-P.; Da Silva, K.-C.-M.; Parrini, S.-C.; Barreiro, E.-J. *Eur. J. Med. Chem.* **1998**, *33*, 189.
24. (a) Svenstrup, S.; Simonsen, K.-B.; Thorup, N.; Brodersen, J.; Dehaen, W.; Becher, J. *J. Org. Chem.* **1999**, *64*, 2814; (b) Abdel-Wahab, B.-F.; Khidre, R.-E.; Farahat, A.-A. *Arkivoc* **2011**, *(i)*, 196; (c) Nagamallu, R.; Srinivasan, B.; Ningappa, M.-B. Kariyappa, A.-K.;

Bioorg. Med. Chem. Lett. **2016**, *26*, 690; (d) Padalkar, V.-S.; Borse, B.-N.; Gupta, V.-D.; Phatangare, K.-R.; Patil, V.-S.; Sekar, N. *J. Heterocyclic Chem.* **2016**, *53*, 1347.

25. Crystallographic Information File for **3a** is included in the Supporting Information.
26. (a) Hong, Y.; Lam, J. W. Y.; Tang, B. Z. *Chem. Soc. Rev.* **2011**, *40*, 5361; (b) Zhang, J. N.; Kang, H.; Li, N.; Zhou, S. M.; Sun, H. M.; Yin, S. W.; Zhao, N.; Tang, B. Z. *Chem. Sci.* **2017**, *8*, 577; (c) Liow, S. S.; Zhou, H.; Sugiarto, S.; Guo, S.; Chalasani, M. L. S.; Verma, N. K.; Xu, J.; Loh, X. J. *Biomacromolecules* **2017**, *18* (3), 886; (d) Chen, X.; Wang, L.; Yang, X.; Tang, L.; Zhou, Y.; Liu, R.; Qu, J. *Sens. Actuator B-Chem.* **2017**, *241*, 1043.
27. National Primary Drinking Water Regulations. https://www.epa.gov/ground-water-and-drinking-water/national-primary-drinking-water-regulations#Inorganic. (Accessed September 22 2017).
28. Frisch, *Æ.*; Frisch, M. J.; Clemente, F. R.; Trucks, G. W. *Gaussian, Inc.: Wallingford, CT* **2009**.
29. (a) Palatinus, L.; Chapuis, G. *J. Appl. Crystallogr.* **2007**, *40*, 786; (b) Sheldrick, G. M. *Acta Crystallogr. Sect. C: Cryst. Struct. Chem.* **2015**, 71, 3.
30. (a) Crosby, G. A.; Demas, J. N. *J. Phys. Chem.* **1971**, *75*, 991; (b) Brouwer, A. M. *Pure Appl. Chem.* **2011**, *83*, 2213; (c) Würth, C.; Grabolle, M.; Pauli, J.; Spieles, M.; Resch-Genger, U. *Nat. Protoc.* **2013**, *8*, 1535; (d) Resch-Genger, U.; Rurack, K. *Pure Appl. Chem.* **2013**, *85*, 2005; (e) Orrego-Hernández, J.; Nuñez-Dallos, N.; Portilla, J. *Talanta* **2016**, *152*, 432.
31. (a) Long, G. L.; Winefordner, J. D. *Anal. Chem.* **1983**, *55*, 712A; (b) Aich, K.; Goswami, S.; Das, S.; Mukhopadhyay, C. D. *RSC Adv.* **2015**, *5*, 31189.
32. Hanwell, M. D.; Curtis, D. E.; Lonie, D. C.; Vandermeersch, T.; Zurek, E.; Hutchison, G. R. *J. Cheminform.* **2012**, *4*, 17.